ResearchGate

See discussions, stats, and author profiles for this publication at: https://www.researchgate.net/publication/331050001

Beijing urban particulate matter-induced injury and inflammation in human lung epithelial cells and the protective effects of fucosterol from Sargassum binderi (Sonder ex J. Agardh…

Article *in* Environmental Research · February 2019

DOI: 10.1016/j.envres.2019.02.016

CITATIONS
31

READS
92

11 authors, including:

Shanura Fernando
Chonnam National University
92 PUBLICATIONS **1,117** CITATIONS
SEE PROFILE

Thilina U. Jayawardena
Jeju National University
48 PUBLICATIONS **287** CITATIONS
SEE PROFILE

Hyun-Soo Kim
122 PUBLICATIONS **913** CITATIONS
SEE PROFILE

A.P.J.P. Vaas
University of Tasmania
6 PUBLICATIONS **53** CITATIONS
SEE PROFILE

Some of the authors of this publication are also working on these related projects:

Project Investigation of soft coral natural products from Jeju Sea, South Korea for their bioactive potential. View project

Project Developing alginate based microspheres/nanospheres View project

All content following this page was uploaded by Chandrika Nanayakkara on 16 March 2019.

The user has requested enhancement of the downloaded file.

Environmental Research 172 (2019) 150–158

Contents lists available at ScienceDirect

Environmental Research

journal homepage: www.elsevier.com/locate/envres

Beijing urban particulate matter-induced injury and inflammation in human lung epithelial cells and the protective effects of fucosterol from *Sargassum binderi* (Sonder ex J. Agardh)

I.P. Shanura Fernando[a], Thilina U. Jayawardena[a], Hyun-Soo Kim[a], Won Woo Lee[a,d], A.P.J.P. Vaas[b], H.I.C. De Silva[b], G.S. Abayaweera[b], C.M. Nanayakkara[c], D.T.U. Abeytunga[b], Dae-Sung Lee[e], You-Jin Jeon[a,*]

[a] Department of Marine Life Science, Jeju National University, Jeju 63243, Republic of Korea
[b] Department of Chemistry, University of Colombo, Colombo 3, Sri Lanka
[c] Department of Plant Sciences, University of Colombo, Colombo 3, Sri Lanka
[d] Freshwater Bioresources Utilization Division, Nakdonggang National Institute of Biological Resources, Sangju 37242, Republic of Korea
[e] Deprartment of Applied Research, National Marine Biodeversity Institute of Korea, 75, Jangsan-ro 101-gil, Janghang-eup, Seocheon, Republic of Korea

ARTICLE INFO

Keywords:
Fine dust
Airway inflammation
A549
Sargassum binderi
Fucosterol

ABSTRACT

Particulate matter (PM) air pollution has gradually become a widespread problem in East Asia. PM may cause unfamiliar inflammatory responses, oxidative stress, and pulmonary tissue damage, and a comprehensive understanding of the underlying mechanisms is required in order to develop effective anti-inflammatory agents. In this study, fine dust collected from Beijing, China (CPM) (size < PM13 with majority < PM2.5) was evaluated for its oxidative stress- and inflammation-inducing effects, which cause cell damage, in A459 human lung epithelial cells. Oxidative stress was marked by an increase in intracellular ROS levels and the production of antioxidant enzymes such as superoxide dismutase (SOD), catalase (CAT), and heme oxygenase-1 (HO-1). Upon induction of oxidative stress, a marked increase was observed in the expression of key inflammatory mediators such as COX-2 and PGE_2 and the pro-inflammatory cytokines TNF-α and IL-6 via NF-kB and MAPK pathways. Cellular damage was marked by a reduction in viability, increased lactate dehydrogenase (LDH) release, formation of apoptotic and necrotic bodies, accumulation of sub-G1 phase cells, and DNA damage. Apoptosis was found to be mediated via the activation of caspases through the mitochondria-mediated pathway. Fucosterol, purified from the brown alga *Sargassum binderi* (Sonder ex J. Agardh) by bio-assay-guided fractionation and purification, exhibited potential therapeutic effects against CPM-induced detrimental effects. Further studies could focus on developing fucosterol, in forms such as steroidal inhalers, against PM-induced pulmonary tissue inflammation.

1. Introduction

Air pollution in China, Korea, and Japan due to fine dust is rapidly turning into a tragedy, with several deleterious effects on human health as well as regional and global climate change. Beijing, the capital of China, is at the center of these calamitous events. Vast amounts of particulate matter (PM) originate primarily during the spring season, with dust storms coming from the Loess Plateau, desert regions of Mongolia, and northwest China (Zhuang et al., 2001). The condition is further aggravated by regional and local emissions from heavily industrialized zones, vehicles, and coal burning. Beijing is considered the most heavily polluted (air) city in the world (Wang et al., 2009). Much attention was focused on this issue when Beijing hosted the 2008 Olympic Games. Since then, stringent steps have been implemented to reduce the level of air pollution in Beijing (Wang et al., 2009). Based on ground measurements, a high proportion of the particulate matter was found to have an aerodynamic diameter of 2.5 μm, with the major components being mineral dust, organic pollutants such as polycyclic aromatic hydrocarbons (PAH), and inorganic components such as sulfate, elemental carbon, nitrate, and ammonium (Huang et al., 2006). An excellent review regarding the fluctuation in $PM_{2.5}$ level in Beijing and its environmental impact is presented by Lv et al. (2016).

Many epidemiological studies indicate that these particulate matters can be absorbed into the lungs, causing severe tissue damage and

* Corresponding author.
E-mail addresses: youjinj@jejunu.ac.kr, youjin2014@gmail.com (Y.-J. Jeon).

https://doi.org/10.1016/j.envres.2019.02.016
Received 5 November 2018; Received in revised form 9 February 2019; Accepted 11 February 2019
Available online 12 February 2019
0013-9351/ © 2019 Elsevier Inc. All rights reserved.

cardiopulmonary complications. Asthma is one such chronic non-communicable inflammatory disease of the respiratory pathway caused by air pollutants. According to revised WHO estimates in August 2017, nearly 235 million people worldwide suffer from asthma. The inhaled PM may provoke allergic inflammation, and is considered the most prominent risk factor for asthma (Nunes et al., 2017). Wang et al. (2002) showed that a major portion of PM (more than 70%) gets deposited below the trachea of the respiratory tract, while nearly 22% reaches the alveoli. This could increase the oxidative stress in the epithelial cell lining in the respiratory tract and other lung tissues, resulting in injury and inflammation (Schaumann et al., 2004; Wang et al., 2009). Some key indicators of cellular stress responses are increased ROS, catalase (CAT), heme oxygenase-1 (HO-1), superoxide dismutase (SOD), and glutathione peroxidase (GPX) (Ighodaro and Akinloye, 2017). Onset of inflammatory responses is marked by increased levels of pro-inflammatory cytokines and inflammatory mediators (Pozzi et al., 2003). A study conducted in Germany suggested that ambient particles released from industries in Hettstedt town are the primary cause of allergic asthma in the children living there (Schaumann et al., 2004). These particles have been found to cause lung inflammation with an increased influx of monocytes. Increased levels of ROS and cytokine (IL-6 and TNF-α) production have also been observed in bronchoalveolar lavage cells.

The public awareness regarding PM has increased over time, and many studies are trying to find ways to counteract the detrimental health impact of PM-induced inflammation and tissue damage. Marine bioactive metabolites have gained increased attention during the recent years as potential drug candidates against a variety of diseases (Sanjeewa et al., 2018). We previously reported the effectiveness of diphlorethohydroxycarmalol from *Ishige okamurae* against the inflammatory responses induced by PM (collected from a road tunnel in Wislostrada, Poland) on keratinocytes and macrophages (Fernando et al., 2017a). Furthermore, alginate purified from *Sargassum horneri* was found to be effective in reducing the toxic metal ion content in PM-induced keratinocytes due to its chelation properties and in lowering the inflammatory responses by inhibiting MAPK/NF-κB pathway mediators (Fernando et al., 2018a). Steroidal anti-inflammatory drugs have long been used for short-term relief and as long-term control agents against asthma, unlike β-adrenoceptor agonists, which can offer only short-term relief. Steroidal drugs work by reducing the mucus production and swelling of the airways caused by inflammatory responses (Barnes, 2010; Donahue et al., 1997). Fucosterol is well known for its anti-inflammatory, antioxidant, anticancer, antidiabetic, antifungal, hepatoprotective, antihyperlipidemic, antiadipogenic, antihistaminic, anticholinergic, anti-osteoporotic, antiphotodamaging, blood cholesterol reducing, and butyrylcholinesterase inhibitory activities, as well as for its preventive role against blood vessel thrombosis (Ahmed et al., 2016). To our knowledge, no study has reported the anti-inflammatory effect of fucosterol on A549 immortalized alveolar basal epithelial cells. The present study was undertaken to identify the impact of PM from Beijing, its mechanism of action, and to explore preventive means to counteract its detrimental effects using fucosterol purified from *Sargassum binderi*.

2. Materials and methods

2.1. Materials

China fine dust particulate matter (CPM)–certified reference material No. 28–was purchased from the National Institute for Environmental Studies, Ibaraki, Japan. Organic solvents (HPLC grade) were purchased from Fisher Scientific Ltd. (Montreal, Quebec, Canada). Preparative TLC silica gel 60 F_{254} glass plates were purchased from Merck (Darmstadt, Germany). Silica (30–60 mesh), 3-(4,5-dimethylthiazol-2-yl)-2,5-diphenyltetrazolium bromide (MTT), 2′ 7′-dichlorodihydrofluorescein diacetate (DCFH2-DA), acridine orange, and bisBenzimide H 33342 trihydrochloride (Hoechst 33342) were purchased from Sigma-Aldrich (St Louis, MO, USA). Deuterated chloroform was purchased from Cambridge Isotope Laboratories (Andover, MA, USA). Human lung epithelial (A549) cells were purchased from Korean Cell Line Bank (KCLB, Seoul, Korea). RPMI, media, FBS, and penicillin and streptomycin mixture was purchased from Thermo Fisher Scientific (Waltham, MA, USA). CytoTox 96® NonRadioactive Cytotoxicity Assay kit (for LDH assay) was purchased from Promega (Madison, WI, USA). Western blotting antibodies were purchased from Santa Cruz Biotechnology (Ca, USA). Cytokine kits were purchased from Invitrogen (Carlsbad, CA, USA) and R&D Systems (Minneapolis, MN, USA).

2.2. Sample collection extraction and purification of fucosterol

S. binderi samples were collected from the Hikkaduwa coastal area of Sri Lanka in January 2018. Repositories were stored in the Department of Plant Sciences, University of Colombo and Department of Ocean Science, Jeju National University. The samples were washed, freeze-dried, powdered, and successively extracted four times with 70% ethanol. Crude ethanolic extract (SBE) was obtained after evaporating the solvents using a rotary evaporator. SBE was suspended in deionized water and fractionated successively using hexane, chloroform, and ethyl acetate. Based on the bioactivities, the hexane fraction (SBEH) was further resolved into five separate fractions (SBEH1–SBEH5) using silica open column. The column was successively eluted with hexane and ethyl acetate solvent systems (9:1 → 7:3 → 1:1) → ethyl acetate → ethyl acetate and methanol (1:4). The fraction SBEH2 was further resolved into five fractions (SBEH21–SBEH25) in a second silica open column, via successive elution with hexane and ethyl acetate solvent systems (17:3 → 4:1 → 3:1 → 7:3 → 3:2). SBEH22 column eluate was finally resolved in a long silica open column, and the column eluents were collected into 135 test tubes. Based on the results of TLC analysis, the test tubes were pooled into five fractions (F1–F5). Fraction F2 was resolved by preparative TLC, yielding seven consecutive factions (F2A–F2G). Fraction F2D indicated the presence of fucosterol, which was identified as the active metabolite. The detailed bioassay-guided purification process is represented in the Supplementary Figs. 1 and 2. For preparing fucosterol samples for cell culture, fucosterol was first dissolved in DMSO (80 mg/mL) and diluted with RPMI culture media as necessary. DMSO concentration in the samples was less than 1%. The samples were stored at −20 °C until treatment.

2.3. Fucosterol structure characterization

The structure of fucosterol was confirmed by GC-MS/MS using a Shimadzu GCMS-TQ8040 system (Shimadzu Corp., Kyoto, Japan) (Fernando et al., 2017b), FTIR (Thermo Scientific NicoletTM 6700 FTIR, MA USA), and a 400-MHz NMR spectrometer (JNM-ECX400, JEOL, Japan) (Fernando et al., 2017c).

2.4. Cell culture

A549 cells were cultured in RPMI media supplemented with 10% FBS and 1% penicillin/streptomycin mixture at 37 °C, under a humidified atmosphere with 5% CO_2. The cells were periodically subcultured, and cells under exponential growth were used for the experiments.

2.5. Evaluation of oxidative stress and cellular damage

CPM was suspended in RPMI media at a stock concentration of 8 mg/mL, mixed using a vortex, and sonicated to eliminate any microbial contamination. The stock solutions were stored at −20 °C until treatment, and necessary dilutions were carried out using RPMI media. Cells (A459) were seeded in 24-well plates (1×10^5 cells mL^{-1}) for 24 h. Different concentrations of CPM were then added to separate

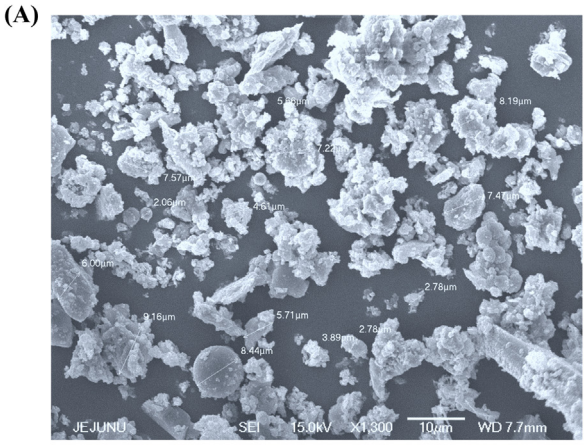

(B)

Element	Mass fraction (ppm)
Na	7960.0 ± 650.0
Mg	14000.0 ± 600.0
Al	50400.0 ± 1000.0
K	13700.0 ± 600.0
Ca	66900.0 ± 2400.0
Ti	2920.0 ± 330.0
Fe	29200.0 ± 1700.0
Zn	1140.0 ± 100.0
V	73.2 ± 7.0
Mn	686.0 ± 42.0
Ni	63.8 ± 3.4
Cu	104.0 ± 12.0
As	90.2 ± 10.7
Sr	469.0 ± 16.0
Cd	5.6 ± 0.4
Ba	874.0 ± 65.0
Pb	403.0 ± 32.0
U	4.3 ± 0.3

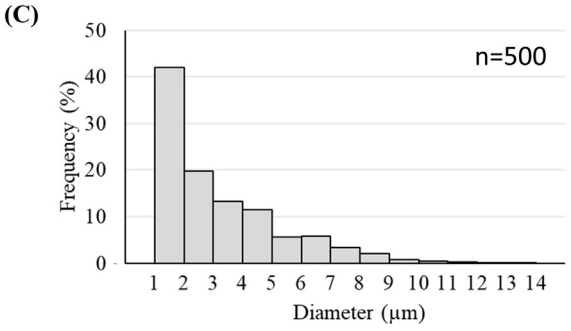

(D)

Component	Amount (ppm)
Fluoranthene	7.00
Pyrene	4.00
Benz[a]anthracene	2.00
Benzo[b]fluoranthene	11.00
Benzo[k]fluoranthene	2.00
Benzo[a]pyrene	0.90
Benzo[ghi]perylene	2.00
Indeno[1,2,3-cd]pyrene	3.00

Fig. 1. Characteristics of Chinese fine dust (CPM). (A) Scanning electron microscopic analysis. (B) The composition of metallic elements. (C) Particle size distribution. (D) Composition of polycyclic aromatic hydrocarbons (PAH). Parts of the figure are reprinted from Fernando et al. (2018a), with permission from Elsevier.

wells. The final volume for each well was 500 μL, and the incubation was carried out for 24 h (final CPM concentration: 3.125–400 μg mL^{-1}). Vials containing CPM were vortexed and re-suspended prior to each treatment, to ensure equalized distribution. Wells were then rinsed twice with RPMI media and added with fresh media along with MTT, to determine the cell viability (Wang et al., 2017). LDH assay was carried out using a commercial kit, in accordance with the manufacturer's instructions. The intracellular ROS levels were estimated using separate 24-h pre-seeded 24-well culture plates. Here, the cells were exposed to CPM for 24 h. Afterwards, the wells were rinsed twice with RPMI media and fresh media was added to the wells. Intracellular ROS levels were estimated by the DCF-DA assay (Wang et al., 2017). These experiments were carried out to optimize the CPM concentration that could significantly affects the cell viability and ROS levels.

To determine the effectiveness of fucosterol, pre-seeded plates were treated with different concentrations of fucosterol and stimulated with CPM (100 μg mL^{-1}) after 1 h. After a 24-h incubation period, the wells were rinsed twice with fresh RPMI media to wash away the CPM particles. Cells were subjected to a variety of assays to determine cell viability, apoptotic body formation (fluoresce staining), and DNA damage (comet assay), as well as flow cytometric analysis of cell cycle phases by propidium iodide staining method. The methods were adopted from our previous study (Fernando et al., 2017b). Above experimental conditions were optimized based on preliminary empirical evaluations.

2.6. Evaluation of inflammatory responses

After fucosterol treatment and CPM (100 μg mL^{-1}) stimulation, the cells were incubated for a 24-h period. The cell culture media from each well were retrieved into Eppendorf centrifuge tubes and centrifuged using a benchtop mini centrifuge for 5 min to remove any interfering CPM. The culture media was used for the determination of prostaglandin E2 (PGE_2) and pro-inflammatory cytokines, including tumor necrosis factor (TNF)-α, Interleukin (IL)-1β, and IL-6. The analysis was done using commercial ELISA kits, according to the manufacturer's instructions. The molecular mediator levels were calculated using the following equation:

Percentage expression = (Absorbance of test well / Average absorbance of CPM treated wells) × 100

2.7. Western blot analysis

Western blot analysis was carried out to evaluate several key molecular mediators that regulate antioxidant defense, inflammatory responses, and mitochondria-mediated apoptosis. After fucosterol treatment and CPM stimulation, the cells were harvested and lysed using a NE-PER® Nuclear and Cytoplasmic extraction kit (Thermo Scientific, Rockford, USA), to obtain nuclear and cytoplasmic proteins. Western blot analysis was carried out according to the method described by (Fernando et al., 2017b).

2.8. Statistical analysis

All quantifiable data are expressed as means ± SD, based on at least three independent replicates. Significant differences among data means were determined using one-way ANOVA followed by Duncan's multiple range test in IBM SPSS Statistics 20 software. P values less than 0.05 ($P < 0.05$) "*" and less than 0.01 ($P < 0.01$) "**" were considered significant.

3. Results

3.1. CPM characterization

Protocol for CPM collection and filtering by mechanical vibration, as well as its detailed chemical composition have been previously

reported by Mori et al. (2008). The chemical composition of metallic elements and PAH are reproduced in Fig. 1(B) and (D) with permission. We also carried out a scanning electron microscopic evaluation for the particle size distribution (Fig. 1(A) and (C)), and found that the particles had a diameter range of 1–14 μm, with the majority being less than 5 μm in diameter.

3.2. Purification, yield, and structural characterization of fucosterol

Purification was carried out by bioassay-guided evaluation of its protective effects against CPM induced inflammation. The process was monitored by TLC. Details of the process are provided in the Supplementary materials (Supplementary Figs. 1 and 2). Fucosterol was isolated as a white color powder. The fucosterol yield was estimated as 0.18% of the dry algal weight by GC-MS/MS, using cholesterol as the reference standard. The melting temperature was estimated as 118.7 ± 1.2 °C. As shown in Supplementary Fig. 5, the molecular ion peak observed at 412.30 agrees with the theoretical molecular mass of fucosterol (412.69 g mol^{-1}). In addition, the fragmentation pattern indicated similarities with the library spectrum (NIST 17 and Wiley 11). The ^{1}H (Supplementary Fig. 3) and ^{13}C NMR (Supplementary Fig. 4) spectra show a resemblance to the fucosterol spectra reported by Majik et al. (2015). Supplementary Fig. 5 indicate predicted mass fragments of fucosterol corresponding to each prominent peak in the MS spectrum.

3.3. Effects on cell viability and oxidative stress induced by CMP

As shown in Fig. 2(A) and (D), increasing CPM treatment concentrations caused a reduction in cell viability compared to the control with late apoptotic bodies appearing at concentrations > 100 μg mL^{-1}. Simultaneously, the ROS levels increased in a dose-dependent manner, up to CPM concentration of 100 μg mL^{-1}, after which it started declining (Fig. 2(B)). With increasing CPM concentrations, a steady increase of ROS levels was observed for the FACS analysis using DCFH-DA fluoroprobe (Fig. 2(F)). These observations were consistent with increasing fluorescence observed for intracellular ROS as visualized by DCFH-DA fluorescence staining (Fig. 2(E)). The LDH release indicated a significant enhancement after 200 μg mL^{-1} CPM (Fig. 2(C)), indicating a minor proportion of necrotic cell damage. Based on these results, 100 μg mL^{-1} was selected as the optimal concentration for further evaluations.

3.4. Protective effects of fucosterol against CPM-induced oxidative stress, apoptotic body formation and DNA damage

As depicted in Fig. 3(A), treatment with CPM caused a significant increase in the ROS levels in A549 cells. Simultaneously, CPM treatment caused a loss in cell viability, whereas the fucosterol (50 μg mL^{-1}) treatment ameliorated it to 94.98 ± 1.26% (Fig. 3(B)). Hoechst 33342 staining revealed that the proportion of apoptotic bodies indicated by nuclear condensation and fragmentation was higher in CPM-treated cells (Fig. 3(C)). The appearance of reddish orange color nucleic fragments upon nuclear staining (Fig. 3(D)) with acridine orange and ethidium bromide mixed stain indicated that the cells were in late apoptosis stage. Fucosterol treatment lowered the appearance of apoptotic bodies in a dose-dependent manner. As evident by the comet assay (Fig. 3(F)), CPM elevated DNA damage in A549 cells marked by the comparatively higher tail DNA contents. The tail DNA contents were markedly reduced with dose-dependent fucosterol treatment. These results agree with the results of the cell cycle analysis (Fig. 3(E)), where an increased proportion of the cells were found to be in the Sub-G1 phase upon CPM treatment. Fucosterol treatment was able to recover a good proportion of the cell damage, marked by the gradual reduction in the Sub-G1 cell population.

3.5. Protective effects of fucosterol against CPM-induced apoptosis and DNA damage

Western blot analysis revealed that CPM could induce apoptotic proteins such as Bax, p53, and Caspases-3 and 9 as well as cleavage of Caspases-3 and 9 (Fig. 4(A)). Further, CPM increased the PARP cleavage while downregulating the anti-apoptotic protein, Bcl-xL. These effects could be successfully reversed upon treatment with fucosterol. As depicted in Fig. 4(B), CPM increased the levels of antioxidant enzymes SOD, CAT, and HO-1 in the cytosol, and NRF2 levels in the nucleus. Increasing fucosterol concentrations increased the antioxidant protein expression levels, in a dose-dependent manner, to values higher than those for CPM treatment.

3.6. Effect of fucosterol in reducing inflammatory responses in A549 cells

CPM treatment promptly increased the levels of inflammatory mediators COX-2 (Fig. 5 (A)), PGE_2 (Fig. 5(B)) and pro-inflammatory cytokines, TNF-α, and IL-6 in A549 cells (Fig. 5(C)). Above observations agree with the CPM induced increase of the P65 and P50 nuclear translocation (Fig. 5(E)) and phosphorylation of p38 MAPK, ERK½, and JNK (Fig. 5(D)). The highest increment was observed for TNF-α, which was seven-folds higher than that in the control. The effect of CPM on IL-1β production was not significantly higher than that in the control. Fucosterol lowered the nuclear translocation of P65 and P50 and phosphorylation of p38 MAPK, ERK½, and JNK. Moreover, fucosterol lowered the levels of COX-2, PGE_2, and pro-inflammatory cytokines, TNF-α and IL-6, in a dose-dependent manner.

4. Discussion

Air pollution has a substantial contribution to the development of respiratory diseases. While implementing regulatory measures and environmental protection policies to reduce the anthropogenic contributions to PM emissions, it is necessary to investigate possible treatment methods to counteract PM-induced diseases. In the present study, fucosterol was purified from the marine brown alga, *S. binderi*, harvested from Sri Lanka. Using GC-MS/MS analysis, its fucosterol content was estimated as 0.18% of the dry weight. The bioassay-guided purification process resulted in the isolation of fucosterol, following the reduction of NO production in LPS-stimulated RAW 264.7 macrophages. Purified fucosterol indicated a broad range of anti-inflammatory effects on several cell lines (RAW, BV2, HaCaT, and A549) under LPS stimulation. GC-MS/MS, FTIR, and NMR spectroscopic analyses were carried out to confirm its structure by comparison with the literature. In the GC-MS/MS analysis, the molecular ion was observed at 412.30, which agrees with the theoretical molar mass of 412.69 g mol^{-1}.

The cell line A549 has been long used in pulmonary research as a suitable substituent to primary or stem cells of the alveolar epithelium. It mimics all the major functionalities of primary alveolar type II (ATII) cells, providing consistent and reproducible data, without any of the technical or ethical issues involved in using stem cells (Cooper et al., 2016). The effect of fine dust on A549 has recently been the subject of several excellent studies (Anita et al., 1999; Calcabrini et al., 2004; Gualtieri et al., 2009). Additional references to above claim are provided in supplementary data 7. PM-stimulation primarily initiates cellular responses such as ROS production and inflammation. However, their potency depends on several factors, including the size and composition of PM (Peden and Reed, 2010). The details regarding the particle size and composition of CPM have been reported in our previous study (Fernando et al., 2018a). Briefly, CPM contains particles with a diameter range of 1–14 μm, wherein a large proportion (more than 85%) have a diameter less than 5 μm. These particles are defined by their mineral and polycyclic aromatic hydrocarbon contents (Mori et al., 2008). The chronic complications of persisting inflammatory conditions cause increased mucus production, swelling of the airways,

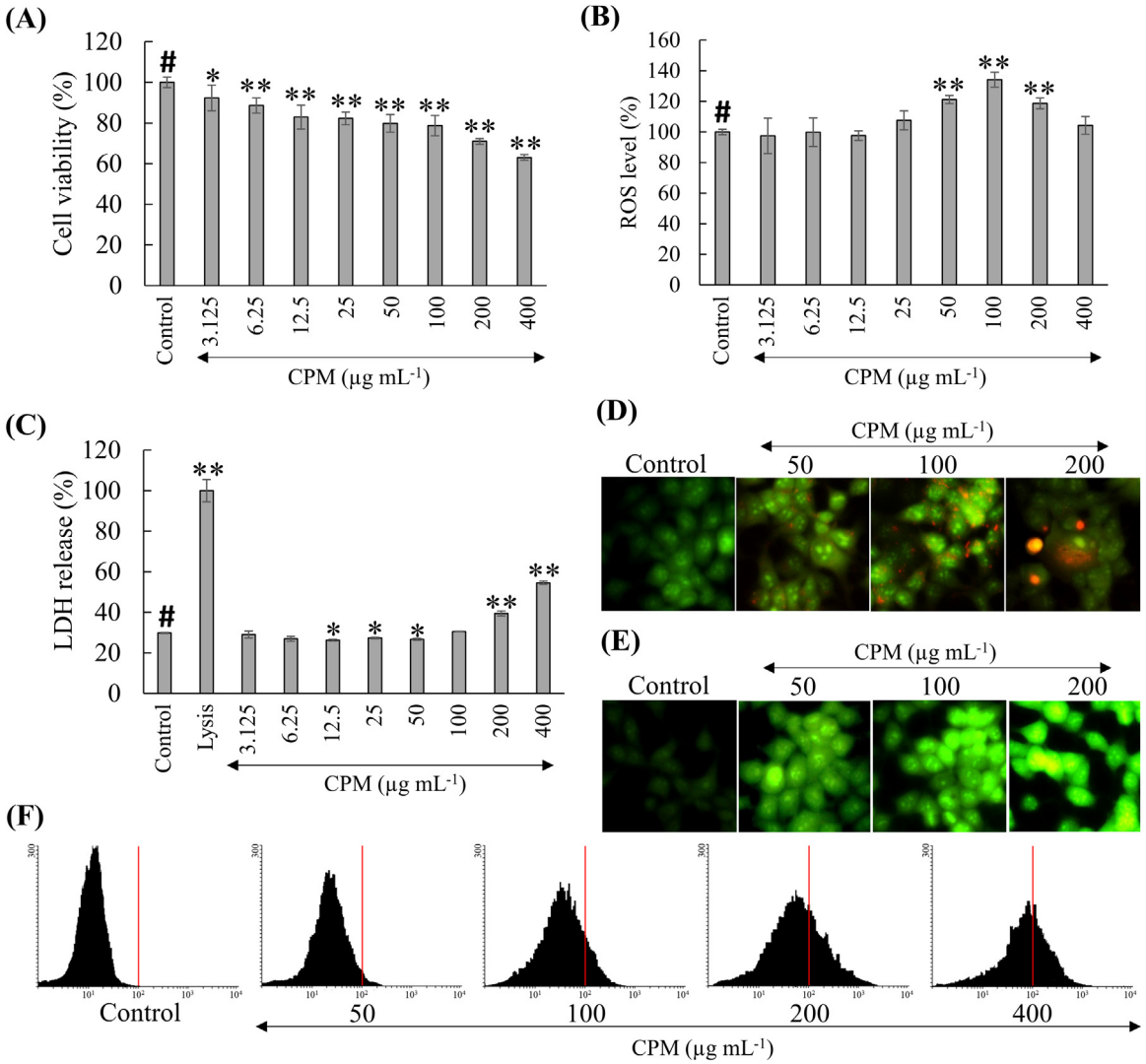

Fig. 2. Dose-dependent effects of CPM on A549 cells. The effect of CPM on (A) cell viability, (B) ROS production, (C) LDH levels, (D) apoptotic body formation and intracellular ROS as visualized by DCFH-DA fluorescence staining (E) and analyzed by FACS (E). These experiments were carried out to identify the optimum concentrations of CPM for further experiments. Data are presented as the means ± SD, based on three independent determinations (n = 3). * $P < 0.05$ and ** $P < 0.01$ were considered significantly different compared with the CPM (only) treatment group (#).

severe damage to lung tissues, and in worst cases, death (Donahue et al., 1997). Preliminary analysis revealed a gradual increase in the ROS level and a decrease in A549 cell viability, upon treatment with CPM concentrations of 3.125–100 μg mL^{-1} for a 24-h period. Concentrations higher than 100 μg mL^{-1} caused severe cell death, leaving a low number of alive cells, which explains the decreased ROS level at 200 μg mL^{-1} CPM concentration. A significant LDH release was observed after 200 μg mL^{-1} concentration, indicating possible necrotic cell damage caused by the loss of membrane integrity (Decker and Lohmann-Matthes, 1988). We selected CPM treatment at 100 μg mL^{-1} for further investigation, as significant ROS production and reduction in cell viability were observed at this concentration.

Treatment with fucosterol at concentrations ranging of 3.125–50 μg mL^{-1} could dose-dependently increase the CPM-induced cell viability up to 94.98 ± 1.26%. However, fucosterol concentrations > 100 μg mL^{-1} caused a minor reduction in CPM-induced cell viability. The observed increase in cell viability could be associated with the reduction in intracellular ROS levels, which are known to cause oxidative stress. The IC_{50} value of fucosterol for reducing CPM (100 μg mL^{-1})-induced ROS production was estimated as 21.74 ± 0.67 μg mL^{-1}. Hence, 12.5 and 25 μg mL^{-1} concentrations of fucosterol were selected for further evaluations. Cytocompatibility data of fucosterol (only) on A549 (Supplementary Fig. 6) also indicate a minor toxicity at 100 μg mL^{-1} concentration for a 24 h incubation period suggesting a threshold dose limitation for the drug.

Cell death can occur via three major routes, i.e. apoptosis, necrosis, and autophagy (Edinger and Thompson, 2004). Apoptosis is an intrinsic cellular suicidal mechanism, regulated by a complex network of signaling pathways. It causes minimum damage to the nearby tissues, as the harmful debris are cleared up by phagocytic cells, preventing the risk of inflammation. Conversely, necrosis is a passive, unorganized cell death strategy, the activation of which causes detrimental consequences such as the induction of inflammation. Necrosis occurs mainly in response to physical damage or agonizing toxic stress. Apoptotic cells can be identified by nuclear condensation, fragmentation, and shrinkage without damage to the plasma membrane (Edinger and Thompson, 2004). In contrast, breakdown of the plasma membrane and vacuolation of the cytoplasm present morphological indications of necrosis. The nuclear double staining method allows characterization of viable cells, as well as cells undergoing early apoptosis, late apoptosis, or necrosis; the respective indications are green homogenous nucleus, fragmented green nucleus, green and orange fragmented nucleus, and homogenous reddish orange color nucleus (Fernando et al., 2017b). Hoechst staining revealed that CPM treatment caused nuclear fragmentation and

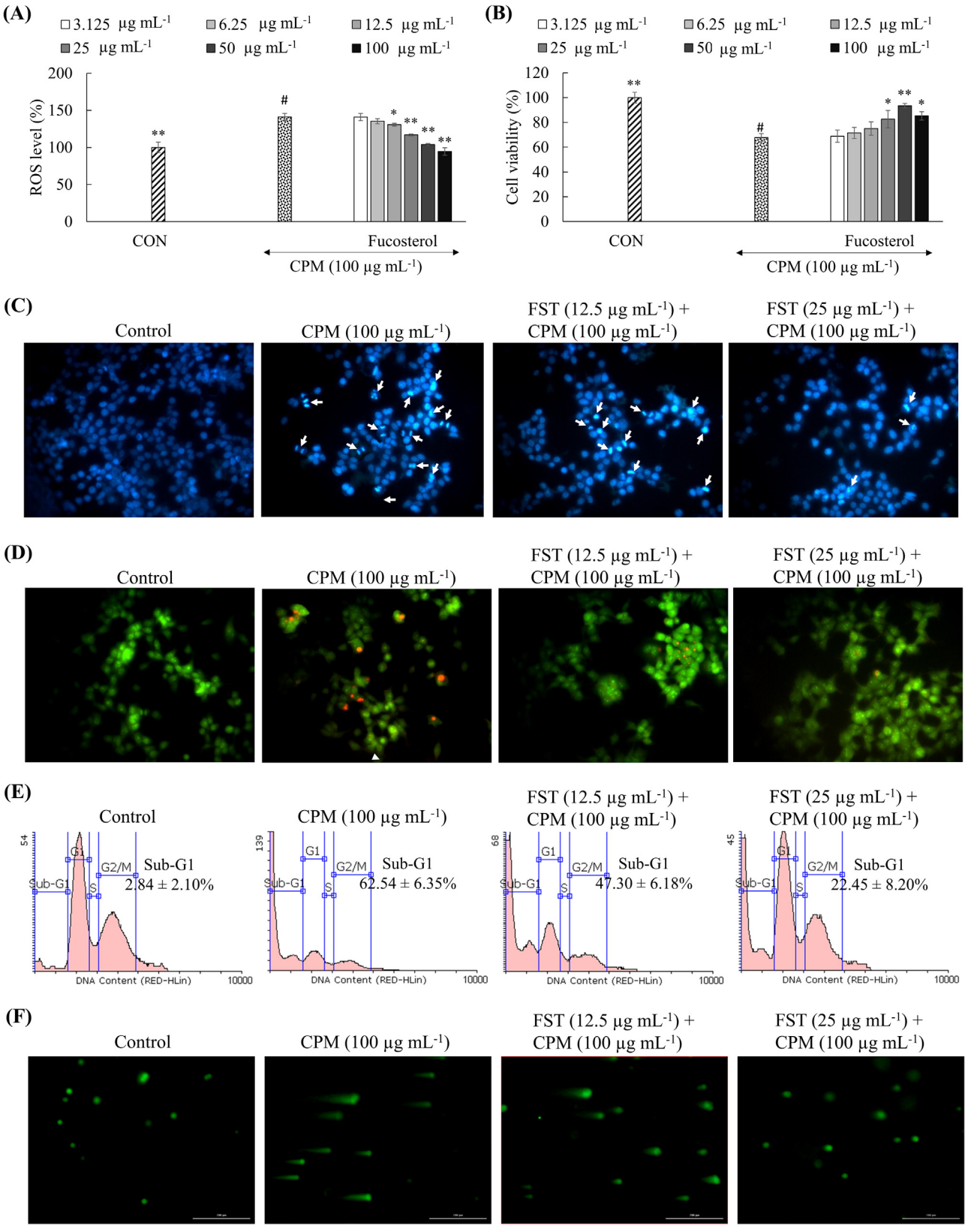

Fig. 3. Effect of fucosterol (FST) on CPM-induced oxidative stress and cell damage. Effect on (A) cell viability, as assessed by MTT assay, and (B) ROS production, as assessed by DCFH-DA assay. Evaluation of apoptotic body formation by (C) Hoechst staining and (D) acridine orange and ethidium bromide mixed stain. (E) Cell-cycle analysis by the propodeum iodide staining method. (F) Comet assay analysis of the DNA damage. Pre-seeded A459 cells (1×10^5 cells mL^{-1}) after 24 h were treated with different fucosterol concentrations for 1 h, induced with CPM, and incubated for 24 h for each analysis. Data presented as the means ± SD, based on three independent determinations (n = 3). * $P < 0.05$ and ** $P < 0.01$ were considered significantly different compared with the CPM (only) treatment group (#).

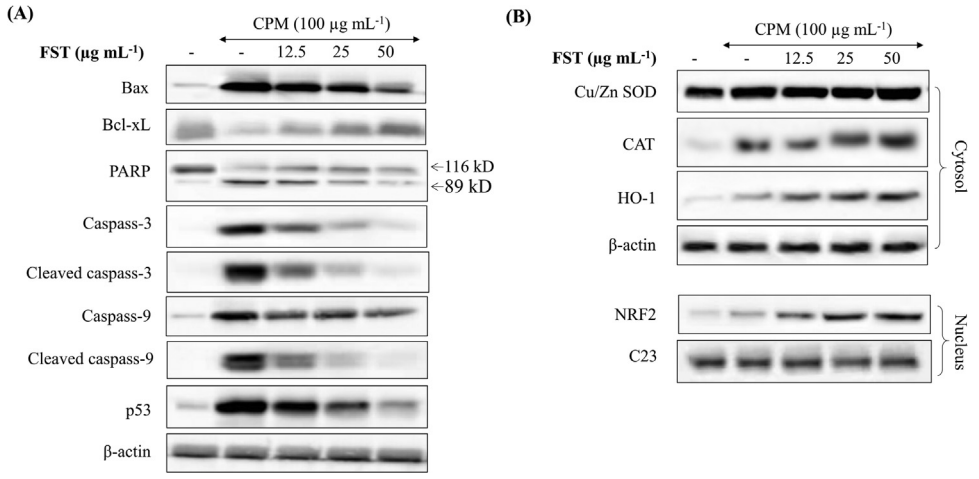

Fig. 4. Effect of fucosterol (FST) on mediating CPM-induced DNA damage in A549 cells mitochondria-mediated apoptotic pathway. Western blot analysis of the molecular mediators of the (A) mitochondria-mediated apoptotic pathway, (B) antioxidant enzyme levels in the cytosol and in the nucleus. Pre-seeded A459 cells (2×10^5 cells mL^{-1}) after 24 h were treated with different fucosterol concentrations for 1 h, induced with CPM, and incubated for 24 h. Harvested cells were used for the comet assay and to obtain proteins for Western blot analysis. Data presented as the means ± SD, based on three independent determinations (n = 3). * $P < 0.05$ and ** $P < 0.01$ were considered significantly different compared with the CPM (only) treatment group.

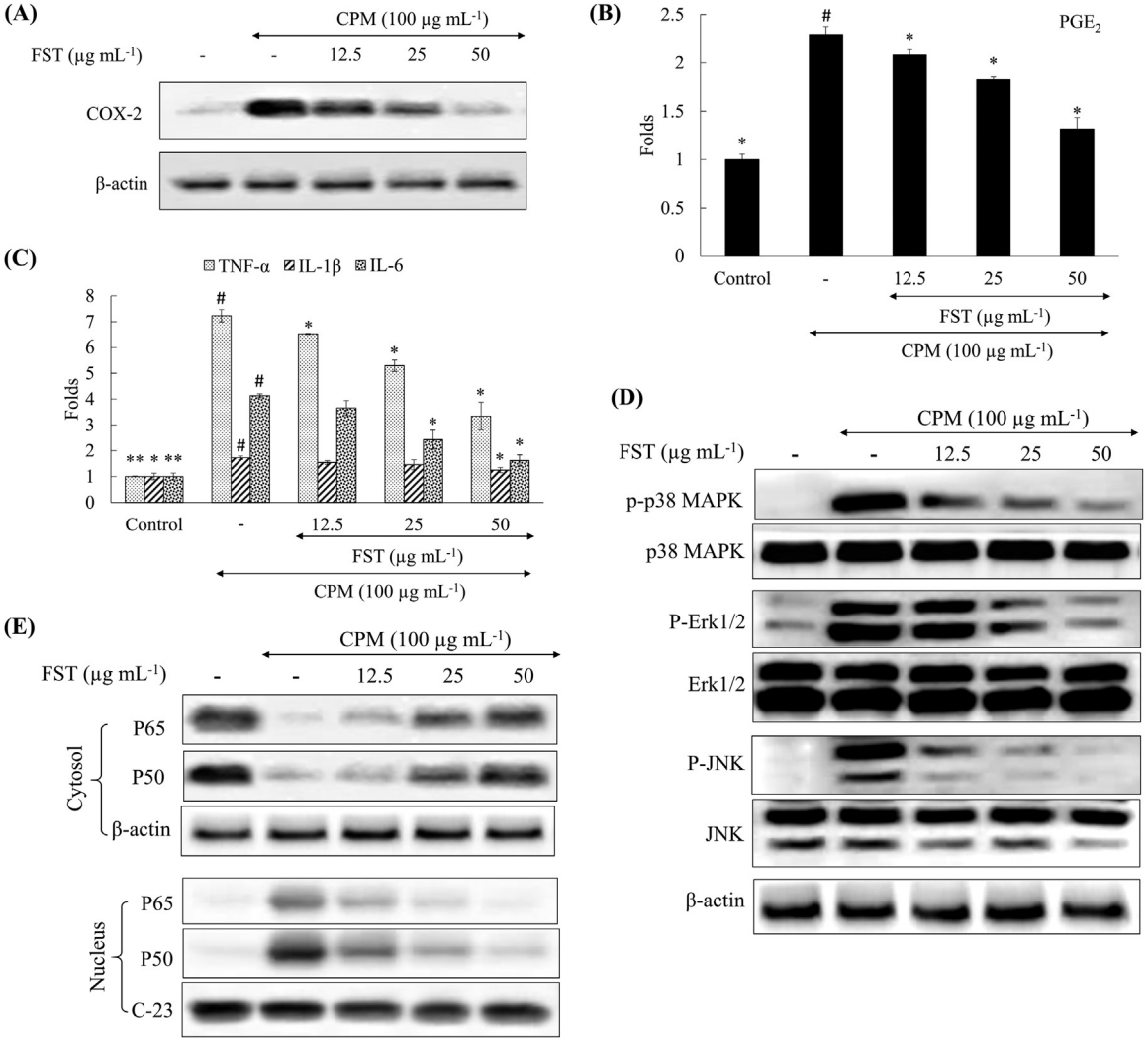

Fig. 5. Inflammation-inducing effects of CPM on A549 cells, and the effect of fucosterol (FST) treatment. (A) Western blot analysis of COX-2 levels, (B) levels of PGE_2 (C) pro-inflammatory cytokines IL-1β, IL-6, and TNF-α, (D) effect on p38 MAPK, ERK½, and JNK phosphorylation, and (E) effect on the nuclear translocation of P65 and P50. Pre-seeded A549 cells (1×10^5 cells mL^{-1}) after 24 h were treated with different fucosterol concentrations for 1 h, induced with CPM and incubated for 24 h. Culture media and harvested cells were used to evaluate the levels of inflammatory mediators and pro-inflammatory cytokines. Data are presented as the means ± SD, based on three independent determinations (n = 3). * $P < 0.05$ and ** $P < 0.01$ were considered significant compared with the CPM (only) treatment group (#).

condensation, marking the formation of apoptotic bodies. Acridine orange and ethidium bromide mixed staining indicated the presence of few necrotic cells in the CPM (only) treated group, whereas a substantial number of cells were in late and early stages of apoptosis. Fucosterol treatment (24 h) led to a complete recovery of cells from necrosis and reduced the occurrence of apoptotic events.

As the next step in investigation, flow cytometry analysis of the cell cycle phases was carried out using the propodeum iodide staining method. A prominent Sub-G1 accumulation was observed for CPM-treated cells, which represents apoptotic hypodiploid cells (Riccardi and Nicoletti, 2006). Fucosterol treatment effectively reduced the Sub-G1 cell populations, indicating its cytoprotective effects. Damage to DNA is another characteristic feature of apoptosis. In the comet assay, the tail DNA percentage represents the extent of DNA damage. CPM-treated A549 cells indicated the highest proportion of DNA damage, whereas fucosterol treatment successfully countered the damage.

Several intracellular antioxidant enzymes, including HO-1, SOD, and CAT, regulate the balance between oxidant and anti-oxidant species in mammalian cells. SOD converts superoxide (O_2^-) radicals to hydrogen peroxide (H_2O_2), and CAT reduces H_2O_2 to H_2O. HO-1 increases the catabolism of heme, a pro-oxidant that mediates the redox chemistry in cells (Fernando et al., 2016). As evident from our Western blot results, CPM increased the levels of SOD, CAT, and HO-1 in A549 cells. Fucosterol further elevated the levels of the above antioxidant enzymes, marking an increase in antioxidant defense. PAH in fine dust has been previously reported to induce ROS production, marked by an increased HO-1 expression and detectable using dithiothreitol assay (Li et al., 2003). The expression of various antioxidant enzymes is regulated mainly by the transcription factor, Nrf2. Nrf2 exists in the cytosol in a bound form with its inhibitor protein, Keap1. Stress conditions activate the Nrf2-dependent cellular defense mechanisms, wherein it detaches from Keap1 and translocates into the nucleus, thereby activating the transcription of cytoprotective genes (Loboda et al., 2016). CPM treatment increased the Nrf2 levels in the nucleus. Fucosterol further elevated the nuclear translocation of Nrf2, indicating that it contributes to strengthening the intracellular antioxidant defense. Previous studies have demonstrated the effect of fucosterol in increasing the expression of antioxidant enzymes SOD catalase and glutathione peroxidase (Lee et al., 2003). Nevertheless, further studies are required to investigate the upstream effect of fucosterol on Nrf2 expression.

Further evaluations were carried out to investigate the levels of some key molecular mediators such as Bcl-2 family proteins and caspases, which could be responsible for regulating apoptosis. A description of their roles has been provided in our previous study (Fernando et al., 2017b). In brief, Bax disrupts ion channels in the mitochondria membrane, causing the release of pro-apoptotic factors and cytochrome c. This activates caspases such as caspase-8 and -9, which, in turn, activate the effector caspases (caspase-3, -6, and -7) that mediate the biochemical and morphological changes during apoptosis. In particular, the effector caspases proteolyze some key structural and regulatory proteins such as PARP, resulting in DNA breakage. Bcl-xL, on the other hand, is an anti-apoptotic protein that inhibits the release of cytochrome c from mitochondria. Observations in this study indicated that CPM could initiate apoptosis via mitochondria-mediated pathway, marked by the increased levels of Bax, caspases −9 and −3, and PARP, and decreased levels of Bcl-xL. Detection of caspase-cleaved fragments is another indication of cells undergoing apoptosis. The expression levels of these molecular mediators could be successfully countered by dose-dependent fucosterol treatment.

As suggested by Edinger and Thompson (2004), inflammation contributes to oxidative stress-induced apoptosis. Especially in the face of necrosis, there is a rapid upregulation of pro-inflammatory cytokine production. As described by Kim et al. (2016), the upstream NF-κB and MAPK signaling pathways mediate the ROS-induced inflammation. These include activation of molecular mediators such as NF-κB p50-p65 complex (related to NF-κB pathway) and ERK1/2, JNK, and p38 (related to MAPK pathway) which in turn activate transcription factors such as p50, p65, and AP-1. Inflammatory cytokines such as TNF-α, IL-1α, IL-1β, IL-6, and IL-8 are synthesized as a result of the nuclear translocation of these activated transcription factors. A graphical representation of this pathway is provided in our previous study (Fernando et al., 2018b). Though A549 is not a cell line belongs to immune system, it has been extensively studied for assessing inflammatory-responses upon PM exposure (Anita et al., 1999; Calcabrini et al., 2004). Supplementary materials section 7 (Supplementary data 7) lists up references to support this claim.

Our results indicated that CPM treatment activated the NF-kB and MAPK molecular mediators which significantly increased the levels of inflammatory mediators PGE_2 and COX-2, and pro-inflammatory cytokines TNF-α and IL-6, all of which were successfully reduced by the fucosterol treatment. PM air pollution has been reported not only in the East Asian region, but from several other places worldwide. However, the size and composition of PM, and its effects on epithelial tissues may vary greatly across different regions. Hence, there is an urgent need for a standardizing measure of the severity of PM. Based on our previous studies and current results, the expression levels of prominent molecular mediators such as TNF-α and IL-6 could serve as potential biomarkers to measure the severity of PM exposure.

In conclusion, an improved understanding of CPM-induced cellular responses and their underlying mechanisms would be beneficial for developing effective drugs to counteract the detrimental effects of PM. Fucosterol purified from *S. binderi* indicated a broad range of effectiveness against CPM-induced ROS production, inflammatory responses, and cell damage, which strengthens the case for its use as a potential candidate for the treatment of fine dust-induced airway alveolar epithelial cell inflammation, cell damage, and asthma. Steroidal anti-asthmatic inhalers are widely used today to counteract inflammatory and allergic responses in the airway epithelial tissues. Further studies could focus on developing fucosterol as an anti-asthmatic drug, which could provide relief from fine dust-induced airway complications.

Acknowledgments

This research was supported by a grant from the Marine Biotechnology Program (20170488) funded by the Ministry of Oceans and Fisheries, Korea.

Appendix A. Supporting information

Supplementary data associated with this article can be found in the online version at doi:10.1016/j.envres.2019.02.016.

References

Ahmed, A.Q., et al., 2016. Health benefit of fucosterol from marine algae: a review. J. Sci. Food Agric. 96, 1856–1866.
Anita, S., et al., 1999. House dust induces IL-6 and IL-8 response in A549 epithelial cells. Indoor Air 9, 219–225.
Barnes, P.J., 2010. New therapies for asthma: is there any progress? Trends Pharmacol. Sci. 31, 335–343.
Calcabrini, A., et al., 2004. Fine environmental particulate engenders alterations in human lung epithelial A549 cells. Environ. Res. 95, 82–91.
Cooper, J.R., et al., 2016. Long term culture of the A549 cancer cell line promotes multilamellar body formation and differentiation towards an alveolar type II pneumocyte phenotype. PLoS One 11, e0164438.
Decker, T., Lohmann-Matthes, M.-L., 1988. A quick and simple method for the quantitation of lactate dehydrogenase release in measurements of cellular cytotoxicity and tumor necrosis factor (TNF) activity. J. Immunol. Methods 115, 61–69.
Donahue, J.G., et al., 1997. Inhaled steroids and the risk of hospitalization for asthma. JAMA 277, 887–891.
Edinger, A.L., Thompson, C.B., 2004. Death by design: apoptosis, necrosis and autophagy. Curr. Opin. Cell Biol. 16, 663–669.
Fernando, I.P.S., et al., 2018a. Anti-inflammatory potential of alginic acid from Sargassum horneri against urban aerosol-induced inflammatory responses in keratinocytes and macrophages. Ecotoxicol. Environ. Saf. 160, 24–31.
Fernando, I.P.S., et al., 2017a. Inhibition of inflammatory responses elicited by urban fine

dust particles in keratinocytes and macrophages by diphlorethohydroxycarmalol isolated from a brown alga Ishige okamurae. Algae 32, 261–273.
Fernando, I.P.S., et al., 2018b. 3[small beta]-Hydroxy-[capital Delta]5-steroidal congeners from a column fraction of Dendronephthya puetteri attenuate LPS-induced inflammatory responses in RAW 264.7 macrophages and zebrafish embryo model. RSC Adv. 8, 18626–18634.
Fernando, I.P.S., et al., 2017b. Apoptotic and antiproliferative properties of 3β-hydroxy-Δ5-steroidal congeners from a partially purified column fraction of Dendronephthya gigantea against HL-60 and MCF-7 cancer cells. J. Appl. Toxicol. 38, 527–536.
Fernando, I.P.S., et al., 2017c. A fucoidan fraction purified from Chnoospora minima; a potential inhibitor of LPS-induced inflammatory responses. Int. J. Biol. Macromol. 104, 1185–1193.
Fernando, P.M.D.J., et al., 2016. Photo-protective effect of sargachromenol against UVB radiation-induced damage through modulating cellular antioxidant systems and apoptosis in human keratinocytes. Environ. Toxicol. Pharmacol. 43, 112–119.
Gualtieri, M., et al., 2009. Winter fine particulate matter from Milan induces morphological and functional alterations in human pulmonary epithelial cells (A549). Toxicol. Lett. 188, 52–62.
Huang, X.-F., et al., 2006. Annual variation of particulate organic compounds in PM2.5 in the urban atmosphere of Beijing. Atmos. Environ. 40, 2449–2458.
Ighodaro, O.M., Akinloye, O.A., 2017. First line defence antioxidants-superoxide dismutase (SOD), catalase (cat) and glutathione peroxidase (GPX): their fundamental role in the entire antioxidant defence grid. Alex. J. Med.
Kim, K.E., et al., 2016. Air pollution and skin diseases: adverse effects of airborne particulate matter on various skin diseases. Life Sci. 152, 126–134.
Lee, S., et al., 2003. Anti-oxidant activities of fucosterol from the marine algae Pelvetia siliquosa. Arch. Pharmacal Res. 26, 719–722.
Li, N., et al., 2003. Ultrafine particulate pollutants induce oxidative stress and mitochondrial damage. Environ. Health Perspect. 111, 455–460.
Loboda, A., et al., 2016. Role of Nrf2/HO-1 system in development, oxidative stress response and diseases: an evolutionarily conserved mechanism. Cell. Mol. Life Sci. 73, 3221–3247.
Lv, B., et al., 2016. A systematic analysis of PM2.5 in Beijing and its sources from 2000 to 2012. Atmos. Environ. 124, 98–108.
Majik, M.S., et al., 2015. Isolation of stigmast-5,24-dien-3-ol from marine brown algae Sargassum tenerrimum and its antipredatory activity. RSC Adv. 5, 51008–51011.
Mori, I., et al., 2008. Development and certification of the new NIES CRM 28: urban aerosols for the determination of multielements. Anal. Bioanal. Chem. 391, 1997–2003.
Nunes, C., et al., 2017. Asthma costs and social impact. Asthma Res. Pract. 3, 1.
Peden, D., Reed, C.E., 2010. Environmental and occupational allergies. J. Allergy Clin. Immunol. 125, S150–S160.
Pozzi, R., et al., 2003. Inflammatory mediators induced by coarse (PM2.5–10) and fine (PM2.5) urban air particles in RAW 264.7 cells. Toxicology 183, 243–254.
Riccardi, C., Nicoletti, I., 2006. Analysis of apoptosis by propidium iodide staining and flow cytometry. Nat. Protoc. 1, 1458.
Sanjeewa, K.K.A., et al., 2018. Nutrients and bioactive potentials of edible green and red seaweed in Korea. Fish. Aquat. Sci. 21, 19.
Schaumann, F., et al., 2004. Metal-rich Ambient Particles (Particulate Matter2.5) Cause Airway Inflammation in Healthy Subjects. Am. J. Respir. Crit. Care Med. 170, 898–903.
Wang, G., et al., 2002. Measurements of PM10 and PM2.5 in urban area of Nanjing, China and the assessment of pulmonary deposition of particle mass. Chemosphere 48, 689–695.
Wang, L., et al., 2017. Protective effect of gallic acid derivatives from the freshwater green alga Spirogyra sp. against ultraviolet B-induced apoptosis through reactive oxygen species clearance in human keratinocytes and zebrafish. Algae 32, 379–388.
Wang, W., et al., 2009. Atmospheric particulate matter pollution during the 2008 Beijing Olympics. Environ. Sci. Technol. 43, 5314–5320.
Zhuang, G., et al., 2001. The compositions, sources, and size distribution of the dust storm from China in spring of 2000 and its impact on the global environment. Chin. Sci. Bull. 46, 895–900.

View publication stats